

## A Spreadsheet-Based Method for Estimating the Skin Disposition of Volatile Compounds: Application to N,N-Diethyl-*m*-Toluamide (DEET)

Gerald B. Kasting , Matthew A. Miller & Varsha D. Bhatt

To cite this article: Gerald B. Kasting , Matthew A. Miller & Varsha D. Bhatt (2008) A Spreadsheet-Based Method for Estimating the Skin Disposition of Volatile Compounds: Application to N,N-Diethyl-*m*-Toluamide (DEET), Journal of Occupational and Environmental Hygiene, 5:10, 633-644, DOI: [10.1080/15459620802304245](https://doi.org/10.1080/15459620802304245)

To link to this article: <https://doi.org/10.1080/15459620802304245>

 View supplementary material 

 Published online: 04 Aug 2008.

 Submit your article to this journal 

 Article views: 238

 Citing articles: 29 View citing articles 

# A Spreadsheet-Based Method for Estimating the Skin Disposition of Volatile Compounds: Application to N,N-Diethyl-*m*-Toluamide (DEET)

Gerald B. Kasting, Matthew A. Miller, and Varsha D. Bhatt

James L. Winkle College of Pharmacy, University of Cincinnati Academic Health Center, Cincinnati, Ohio

*The disposition of N,N-diethyl-3-methylbenzamide (DEET) applied to split-thickness human cadaver skin was measured in modified Franz cells maintained at 32°C and fitted with a vapor trap. Ethanolic solutions of DEET (1% w/w) spiked with <sup>14</sup>C radiolabel were applied to skin at a dose of 10 µL per cell, corresponding to a DEET dose of 127 µg/cm<sup>2</sup>. Room air was drawn over the skin at velocities ranging from 10–100 mL/min. Evaporation of radiolabel from the skin surface and absorption into the receptor solution were monitored for 24 hr post-dose. The percentage of radioactivity collected in the vapor trap after 24 hr increased with airflow, ranging from 16 ± 4% at 10 mL/min to 59 ± 7% at 70 mL/min. The percentage of radioactivity absorbed through the skin after 24 hours decreased with increasing airflow, ranging from 69 ± 7% at 10 mL/min to 20 ± 1% at 80 mL/min. Tissue retention after 24 hr was 6–14% of the radioactive dose with no clear correlation to airflow. This data as well as DEET absorption data from two previous in vitro studies in which dose and location (fume hood or bench top) was varied were analyzed in terms of a recently developed diffusion/evaporation model for skin implemented on an Excel spreadsheet. A priori model calculations based on independently estimated transport parameters (Model 1) were compared with calculations based on fitted parameters (Models 2 and 3). The analysis of the combined dataset (n = 272 observations) showed that the Model 1 estimates matched the cumulative disposition profiles to within a root mean square error of 12.4% of the applied dose (r<sup>2</sup> = 0.65), whereas the Model 2 and Model 3 fits matched to within 9.4% (r<sup>2</sup> = 0.80) and 6.5% (r<sup>2</sup> = 0.91), respectively. The Model 3 fits were obtained using a concentration-dependent diffusivity of DEET in the stratum corneum, the value of which increased 3.4-fold between low concentrations and saturation. This result was consistent with the mild skin penetration enhancement effect for DEET reported elsewhere.*

[Supplementary materials are available for this article. Go to the publisher's online edition of Journal of Occupational and Environmental Hygiene for the following free supplemental resource: a word document containing tables and figures including more information on the spreadsheet skin absorption model.]

**Keywords** dermal risk assessment, mathematical model, percutaneous absorption, skin penetration

Address correspondence to: Gerald B. Kasting, James L. Winkle College of Pharmacy, University of Cincinnati Academic Health Center, P.O. Box 670004, Cincinnati, OH 45267-0004; e-mail: gerald.kasting@uc.edu.

The present affiliation for Varsha D. Bhatt is Dow Pharmaceutical Sciences, Inc., Petaluma, California.

## INTRODUCTION

A variety of methods exist for estimating the absorption rates of noncorrosive organic liquids contacting the skin. An easily applied and useful approximation is to calculate the maximum flux from aqueous solution as the product of skin permeability coefficient ( $k_p$ ) and water solubility ( $S_w$ ) and assume that flux of the neat liquid will be comparable.<sup>(1)</sup> Mathematically,

$$J_{\max} = k_p S_w \quad (1)$$

where the flux  $J_{\max}$  is implicitly taken to be the absorption rate per unit area. Absorbed amount  $M$  may then be estimated as

$$M = J_{\max} A \cdot t_{\text{exp}} \quad (2)$$

where  $A$  is the exposed surface area and  $t_{\text{exp}}$  is the skin contact or exposure time. This method has the merit of simplicity and the fact that suitable values of  $k_p$  and  $S_w$  are easily found or estimated.<sup>(2–6)</sup> There is even a fortuitous cancellation of errors because the moderate skin penetration enhancement provided by high concentrations of many low molecular weight organic liquids<sup>(7,8)</sup> is compensated by the moderate enhancement imparted by skin hydration.<sup>(9,10)</sup> The utility of steady-state skin permeability models in dermal risk assessment for systemic exposure was summarized by Wilschut and colleagues.<sup>(11)</sup> More recently, their use in skin sensitization risk assessment has been discussed.<sup>(1)</sup>

Drawbacks to the steady-state approach include the lack of any information regarding the time course of absorption and, for finite doses of volatile liquids, the lack of guidance as to the expected skin contact time. More sophisticated approaches have been reported<sup>(12,13)</sup> and remain under

development.<sup>(14,15)</sup> The challenge with the latter approaches, which involve the solutions to transient diffusion problems, is to make them accessible to the risk assessment practitioner. Analytical tools such as Laplace transform limits<sup>(13,16)</sup> are a useful step in this direction; however, extracting the full-time course information from these solutions generally involves sophisticated mathematics. The analytical solutions become very complicated when additional skin layers or boundary layers are considered.<sup>(16,17)</sup> The analysis described in this article employs a spreadsheet-based computational tool under development in our laboratory. The math in this package is hidden in an Excel workbook and associated add-in; the user works with the spreadsheet interface. The method is exemplified by calculations associated with the disposition of finite doses of N,N-diethyl-3-methylbenzamide (DEET) applied to excised human skin *in vitro*. A new laboratory study involving the impact of airflow on DEET absorption and evaporation is presented and analyzed. Further application of the model to DEET evaporation studies performed in other laboratories<sup>(18,19)</sup> is also presented.

DEET absorption through human skin has been widely studied both *in vitro* and *in vivo*. Much of the information through the mid-1990s is summarized in reviews by Selim et al.<sup>(20)</sup> and Qui et al.<sup>(21)</sup> DEET has been reported to be a penetration enhancer for skin,<sup>(22)</sup> although it may have the opposite effect under some conditions.<sup>(23)</sup> A previous report from our laboratory<sup>(24)</sup> presented human *in vitro* data showing the dose dependence of DEET absorption and discussed the factors affecting its skin absorption in the context of an earlier version of the diffusion model presented here. The analysis showed that DEET was a mild enhancer for both its own absorption and the absorption of benzyl alcohol through skin. The effect of airflow over the diffusion cells was also examined by comparing fume hood and bench top results.

This report presents details of an additional human *in vitro* study in which the airflow above the skin surface was systematically varied and both DEET evaporation and absorption rates were explicitly determined. The analysis differs from that described by Santhanam et al.<sup>(24)</sup> in that the evaporation mass transfer model is more sophisticated and multiple skin layers are included in the model. *A priori* (Model 1) calculations involving no experimentally fitted parameters are compared with calculations employing either a fitted constant diffusivity (Model 2) or a concentration-dependent diffusivity (Model 3) of DEET in the stratum corneum.

## METHODS

### Chemicals

Carbonyl-<sup>[14C]</sup> DEET (52 mCi/mmol) was custom synthesized. The radiochemical purity was stated by the manufacturer to be 99%. Unlabeled DEET, calcium-free Dulbecco's phosphate-buffered saline (PBS), sodium azide, and bovine serum albumin (BSA) were purchased from Sigma-Aldrich (St. Louis, Mo.). Dialysis membrane (6000 MW cutoff) was purchased from Fisher Scientific (Waltham, Mass.). Soluene-

350 was from Perkin-Elmer Biosciences. Ethanol (95%) was from Phamco-AAPER (Brookfield, CT).

### Protein Binding Study

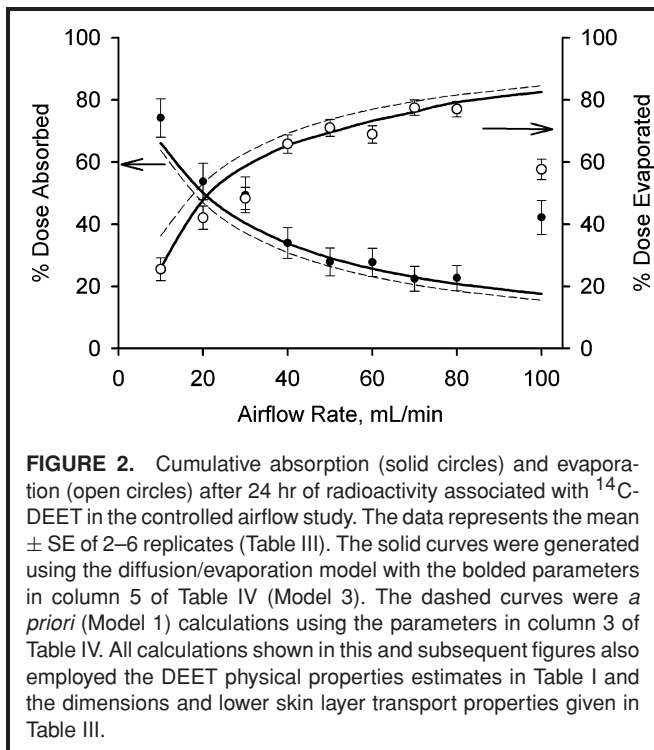
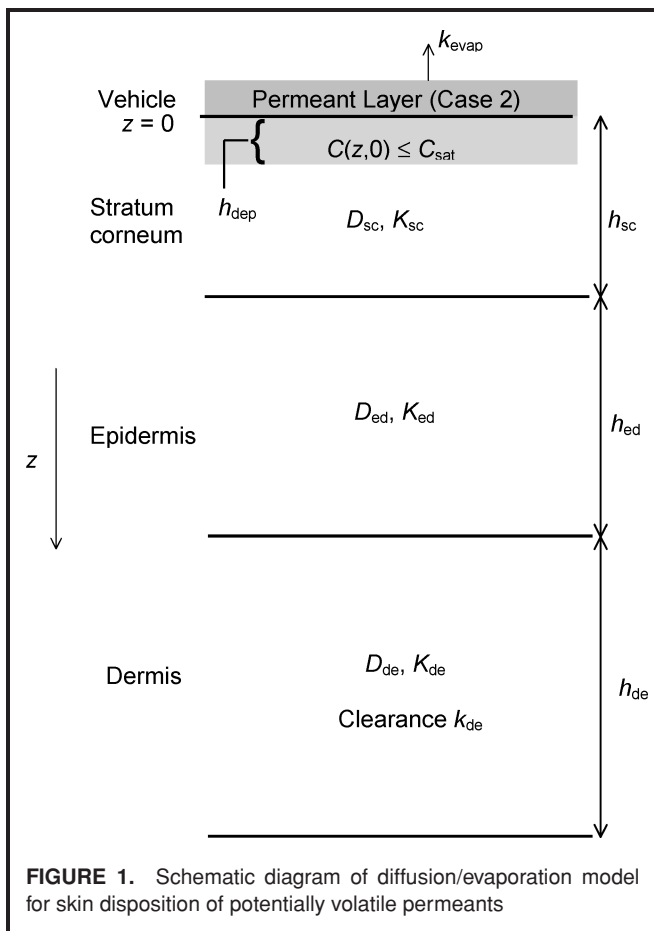
The binding of DEET to albumin was determined by equilibrium dialysis in side-by-side diffusion cells (PermeGear, Hellertown, Pa.). A solution of DEET (10  $\mu\text{g/mL}$ ) containing 0.1  $\mu\text{Ci/mL}$  of [<sup>14</sup>C]-DEET in PBS was placed in the donor compartment, and PBS containing 2% w/v BSA was placed in the receptor compartment. The compartments were separated by a dialysis membrane and maintained at 37°C by a water jacket. Samples (100  $\mu\text{L}$ ) were periodically withdrawn from both compartments, replaced with fresh buffer solution, and analyzed for radioactivity by liquid scintillation counting until equilibrium was reached (about 2–3 days). The fraction of DEET unbound under these conditions ( $f_u$ ) was calculated as the equilibrium ratio of the radioactivity level in the donor solution to that in the receptor solution.

### Controlled Airflow Study

The method has been previously described,<sup>(25)</sup> but the data presented here is new. Ten microliters of a 1% w/w solution of DEET dissolved in ethanol and containing  $\sim 0.5 \mu\text{Ci}$  of [<sup>14</sup>C]-DEET was applied to each 0.79  $\text{cm}^2$ , split-thickness (300  $\mu\text{m}$ ) skin sample mounted on a modified Franz diffusion cell. A total of 2–6 experiments were performed at each airflow, using skin from a single Caucasian donor. A top that allowed for trapping of volatiles under a controlled airflow was quickly fitted to the cell. The specific dose of DEET was thus 127  $\mu\text{g/cm}^2$ . Each joint between components was wrapped with a piece of Parafilm. Room air at ambient temperature and humidity (not measured) was drawn over the samples at controlled flow rates ranging from 10–100 mL/min. These rates correspond approximately to linear velocities ranging from 0.15–2.9 m/s according to the correlation developed in the Data Analysis section (Eq. 7). Thus, they encompass airflows typical of both indoor and outdoor environments.<sup>(26)</sup> The air impinged on the center of the sample from a small inlet tube as depicted in Figure 2 of Reference 25. The angle of incidence was approximately 90° to the skin surface. Volatiles were collected in absorbent cartridges at regular intervals and analyzed (along with the receptor solution samples) by liquid scintillation counting following thermal desorption into 10 mL of scintillation fluid.<sup>(25)</sup> Thermal desorption was carried out for 15 min at 220°C using ultra pure nitrogen gas at a flow rate of 20 mL/min countercurrent to the direction of sorption. At the conclusion of each experiment, the pieces of Parafilm and an ethanol rinse of the upper components of each cell were also collected into vials for scintillation counting.

### Variable Dose Study

The results of this study have been previously reported.<sup>(24)</sup> The method was similar to the controlled airflow study except that conventional, unoccluded tops to the Franz cells were employed, and the diffusion cells were placed either on the bench top or in a fume hood with the sash set at 18 inches.



DEET doses ranging from  $0.02 \mu\text{g}/\text{cm}^2$  to  $11.1 \text{ mg}/\text{cm}^2$  dissolved in ethanol were applied to each split-thickness ( $250 \mu\text{m}$ ; back, thigh or abdominal) skin sample. The results represent the average of three donors, with  $n = 3\text{--}4$  samples per donor. These doses span the range from a trace exposure to a heavy application of a concentrated mosquito-repellent formulation. The dose volume was  $5 \mu\text{L}$  for the smaller doses,  $10 \mu\text{L}$  for the  $8.3 \text{ mg}/\text{cm}^2$  dose, and  $20 \mu\text{L}$  for the  $11.1 \text{ mg}/\text{cm}^2$  dose.

### Location Study

Total absorption from this study, but not the absorption time course, was previously reported.<sup>(24)</sup> The design was similar to the variable dose study except that a single dose of  $117 \mu\text{g}/\text{cm}^2$  of DEET in  $5 \mu\text{L}$  of ethanol was applied to each skin sample. The diffusion cells were located either on a laboratory bench top or in the fume hood. Cadaver skin from a single donor, balanced according to  $^3\text{H}_2\text{O}$  permeability, was used for both locations.

### Diffusion Model

A transient diffusion/evaporation model implemented as an Excel spreadsheet with an associated add-in was used for all calculations. This one-dimensional, multilayer model has been described elsewhere in considerable detail.<sup>(8,12,27–31)</sup> Effective parameters for permeant transport through the slab-like system depicted in Figure 1 were developed from microscopic transport models. The stratum corneum component is based on the work of Nitsche and co-workers<sup>(27–29)</sup> with a deposition layer and volatilization from the skin surface as described by Kasting and Miller.<sup>(12)</sup> The dermis component follows the approach of Kretsos et al.<sup>(32)</sup> Epidermis is treated (at present) as unperfused dermis. Additional details and all the relevant equations may be found in two recent book chapters.<sup>(30,31)</sup>

To run a calculation with the spreadsheet, one enters the physical properties of the test permeant; a vehicle and a specific dose ( $\mu\text{g}/\text{cm}^2$ ); and the environmental factors of wind velocity, skin temperature and skin hydration state. The input parameters for DEET are shown in Table I. After ascertaining the input data is correct and complete, one simply clicks on the “Simulate” button on the add-in toolbar. Graphical and numerical output data is available within a few seconds.

### Data Analysis

Cumulative absorption and evaporation data from all experiments and all conditions within each experiment except for the  $100 \text{ mL}/\text{min}$  airflow condition was analyzed according to the spreadsheet diffusion model. Nonlinear regression analysis was performed within the spreadsheet using a routine from Bevington<sup>(33)</sup> involving a parabolic extrapolation of the  $\chi_v^2$  surface, where  $\chi_v^2$  is the residual sum of squares normalized by the degrees of freedom,

$$\chi_v^2 = \frac{1}{n-p} \sum_{i=1}^n w_i [y_i(\text{obs}) - y_i(\text{fit})]^2 \quad (3)$$

**TABLE I. Physical Properties of DEET at 32°C**

Parameter	Units	Value	Ref.
MW	g/mol	191.3	—
P <sup>A</sup>	g/cm <sup>3</sup>	0.989 <sup>B</sup>	24
log K <sup>C</sup> <sub>oct</sub>		2.18	40
P <sup>D</sup> <sub>vp</sub>	torr	0.00320 <sup>E</sup>	21
S <sup>F</sup> <sub>w</sub>	g/L	9.9 <sup>G</sup>	—
f <sup>H</sup> <sub>u</sub>		0.189	
f <sup>I</sup> <sub>non</sub>		1.00	

<sup>A</sup>Density.

<sup>B</sup>Calculated from reported value of 0.996 at 20°C using an estimated thermal expansivity of 0.0003 K<sup>3/4</sup>.

<sup>C</sup>Octanol/water partition coefficient.

<sup>D</sup>Vapor pressure.

<sup>E</sup>Extrapolated from 25°C value of 0.00167 torr by modified Grange method.<sup>(5)</sup>

<sup>F</sup>Water solubility.

<sup>G</sup>Estimated to be equivalent to 25°C value reported in Qui et al.<sup>(21)</sup>

<sup>H</sup>Fraction unbound in a 2% albumin solution.

<sup>I</sup>Fraction nonionized at pH 7.4.

In Eq. 3,  $n$  is the number of observations,  $p$  is the number of adjustable parameters,  $w_i$  is the weight and the  $y_i$ 's are the cumulative amounts absorbed or evaporated expressed as percentage of dose for each observation. Equal weights ( $w_i = 1$ ) were used for the regression analysis to emphasize cumulative disposition profiles rather than absorption and evaporation rates.<sup>(34)</sup> Data from each experimental study was analyzed separately before combining them into one merged dataset containing 272 observations. Although the merged dataset could not be modeled as precisely as the separate experiments, the parameters arising from the merged analysis were quite stable and did not differ in a physically meaningful way from those obtained via separate analyses. We have therefore reported the merged dataset parameters in the results that follow. The statistical significance of improvements in fit was assessed by an  $F$  test of the  $\chi^2_v$  ratios.<sup>(33)</sup>

Three model variations are reported. Model 1 represents *a priori* calculations made using the default skin transport and partitioning parameters built into the spreadsheet. These parameters derive from a number of sources.<sup>(8,12,27–29,32)</sup> Formulas for their estimation are given in the online supplementary material. Numerical values pertinent to DEET in partially hydrated human skin are listed in Table II. Among the parameters that may be derived from the combination of the underlying dimensional and transport parameters with permeant physical properties are the fractional deposition depth of the permeant in the stratum corneum,  $f_{\text{dep}}$ ; permeant solubility in the stratum corneum,  $C_{\text{sat}}$ ; a saturation dose,  $M_{\text{sat}}$ ; and a volatility parameter,  $\chi$ .<sup>(12)</sup> Formulas are given in Table II. As in a previous analysis of DEET skin disposition,<sup>(24)</sup> the value  $f_{\text{dep}} = 0.1$  was found to be nearly optimum and was used for all analyses. This choice means that the upper 10% of the stratum corneum was considered to be immediately accessible to the permeant following solvent deposition. For

**TABLE II. Parameters for *a priori* (Model 1) Calculation of DEET Absorption Through Partially Hydrated Human Skin *in vitro***

Parameter	Units	Value
Stratum corneum		
$h_{\text{sc}}$	$\mu\text{m}$	13.4
$h_{\text{dep}}$	$\mu\text{m}$	1.34
$D_{\text{sc}}$	$\text{cm}^2\text{s}^{-1}$	$2.91 \times 10^{-11}$
$K_{\text{sc}}$	—	18.42
Viable epidermis		
$h_{\text{ed}}$	$\mu\text{m}$	100
$D_{\text{ed}}$	$\text{cm}^2\text{s}^{-1}$	$8.98 \times 10^{-7}$
$K_{\text{ed}}$	—	1.51
Dermis		
$h_{\text{de}}$	$\mu\text{m}$	400
$D_{\text{de}}$	$\text{cm}^2\text{s}^{-1}$	$8.98 \times 10^{-7}$
$K_{\text{de}}$	—	1.51
$k_{\text{de}}$	$\text{s}^{-1}$	0
Environmental factors		
$T$	$^{\circ}\text{C}$	32
$U$	m/s	0.165 (bench top) 0.72 (fume hood) $(v/44)^{1.282}$ (airflow study)
$k_g$	$\text{cmh}^{-1}$	269 (bench top) 849 (fume hood) $6320 \text{ MW}^{-1/3} u^{0.78}$ (airflow study)
Derived parameters		
$f_{\text{dep}}$	—	Formula <sup>A</sup> $h_{\text{dep}}/h_{\text{sc}}$
$C_{\text{sat}}$	$\text{mg}/\text{cm}^3$	$K_{\text{sc}}S_w$
$M_{\text{sat}}$	$\mu\text{g}/\text{cm}^2$	$h_{\text{dep}}C_{\text{sat}}$
$\chi$	—	$h_{\text{sc}}k_{\text{evap}}\rho/D_{\text{sc}}C_{\text{sat}}$

Note: Formulas for the transport parameters can be found in the online supplementary material.

<sup>A</sup>Ref. 12.

small doses of permeant (doses less than or equal to  $M_{\text{sat}}$ ) the deposition depth concept leads to lower initial evaporation rates and increased percent absorbed, consistent with experimental data for a number of volatile compounds.<sup>(8,12,15,24)</sup>

Models 2 and 3 represent variations on the Model 1 calculations in which the stratum corneum and evaporation mass transfer parameters were fit to the experimental data. These parameters were selected because the stratum corneum contributed more than 98% of the diffusive resistance of the tissue for this moderately lipophilic compound. For Model 2, three parameters were varied:  $D_{\text{sc}}$ ,  $K_{\text{sc}}$  and  $k'_g$ . Here  $k'_g$  is a multiplier for the gas phase mass transfer coefficient defined by the following relationships:

$$J_{\text{evap}}(t) = \begin{cases} k_{\text{evap}}\rho C(0, t)/C_s & \text{Case 1 (small doses)} \\ k_{\text{evap}}\rho & \text{Case 2 (large doses)} \end{cases} \quad (4)$$

$$k_{\text{evap}}\rho = k_g \left[ \frac{P_{\text{vp}}\text{MW}}{(0.76 \times 10^6)RT} \right] \quad (5)$$

$$k_g = k'_g\text{MW}^{-1/3}u^{0.78} \quad (6)$$

In Eqs. 5 and 6,  $P_{vp}$  is permeant vapor pressure in torr, MW is permeant molecular weight and  $u$  is the wind velocity in m/s. For the controlled airflow study the following relationship between  $u$  and airflow in mL/min ( $v$ ) was employed:

$$u = (v/44)^{1.282} \quad 20 \leq v \leq 80 \quad (7)$$

The combination of Eqs. 6 and 7 is equivalent to the statement that

$$k_g = k'_g MW^{-1/3} (v/44) \quad 20 \leq v \leq 80 \quad (8)$$

Thus the evaporation mass transfer coefficient  $k_{evap}$  was considered to vary proportionally to  $v$  in the controlled airflow study. This approximation worked well in previous studies of benzyl alcohol<sup>(25,35)</sup> and was found to be satisfactory for DEET. However, given the limited range of airflows studied, a non-unit exponent for  $v$  in Eq. 8 (cf. Eq. 6) cannot be ruled out.

Model 3 explored the value of allowing a concentration-dependent diffusivity of DEET in the stratum corneum. This choice was motivated by the increased DEET absorption rates at higher doses in the variable dose study and its ability to increase the permeation rates of other compounds.<sup>(24)</sup> A sigmoidal function was arbitrarily chosen to represent  $D_{sc}(C)$  as in Ref. 8; the function employed was

$$D_{sc} = D_0 + \frac{D_{sat} - D_0}{1 + \exp [m (1 - C/C_{trans})]} \quad (9)$$

To limit the flexibility in the fit, the value of  $k'_g$  was fixed at the Model 2 value. The parameters  $D_0$ ,  $D_{sat}$ ,  $C_{trans}$  and  $m$  were varied, as well as the stratum corneum/water partition coefficient  $K_{sc}$ . The procedure was similar to that used previously to describe the penetration enhancement effects of benzyl alcohol.<sup>(8)</sup>

## RESULTS

### Protein Binding Study

The fraction of DEET unbound in a 2% solution of BSA in PBS maintained at 37°C (mean  $\pm$  SD,  $n = 4$ ) was  $f_u = 0.189 \pm 0.008$ . This value was used to estimate the partition coefficient of DEET in viable epidermis and dermis as described elsewhere.<sup>(32)</sup>

### Controlled Airflow Study

The mass balance for radioactivity associated with <sup>14</sup>C-DEET 24 hr following application to the excised skin samples is shown in Table III. Figure 2 shows the estimated percentage absorbed and evaporated plotted versus airflow rate over the skin surface. DEET evaporation increased monotonically with airflow over the range 10–80 mL/min, then decreased abruptly at 100 mL/min. Absorption showed the opposite pattern. Some skin samples were observed to vibrate in the 100 mL/min airstream, indicating a change in the aerodynamics of the system at this high flow rate. Consequently, the 100 mL/min data was excluded from further analyses.

Representative time courses for absorption and evaporation of <sup>14</sup>C-DEET under low (30 mL/min) and high (80 mL/min) airflow conditions are shown in Figure 3. Cumulative data is plotted in the upper panels, and the instantaneous fluxes associated with these curves are shown in the lower panels. The theoretical curves on the graphs are calculated values associated with the diffusion model and described later. The evaporation data (Figures 3a and c) was necessarily measured at the volatiles trap rather than at the skin surface. There was an appreciable time lag associated with this data at the 30 mL/min airflow. In general, the time lag for volatiles collection increased substantially with decreasing airflow,

**TABLE III. Mass Balance for Controlled Airflow Study of <sup>14</sup>C-DEET Disposition on Human Skin *in vitro***

Airflow ( $n$ ), mL/min	A			B		
	Cartridge	Cell Wash <sup>A</sup>	Parafilm	Tissue <sup>B</sup>	Receptor Fluid	Total Recovery
10 (4)	15.8 $\pm$ 3.8	1.2 $\pm$ 0.3	0.7 $\pm$ 0.5	8.0 $\pm$ 2.9	68.8 $\pm$ 6.6	94.5 $\pm$ 1.1
20 (4)	29.1 $\pm$ 5.5	1.4 $\pm$ 0.3	0.0 $\pm$ 0.0	7.4 $\pm$ 0.6	51.8 $\pm$ 6.0	89.7 $\pm$ 5.1
30 (4)	41.3 $\pm$ 10.5	1.9 $\pm$ 0.4	0.4 $\pm$ 0.2	11.9 $\pm$ 4.0	36.7 $\pm$ 9.7	92.2 $\pm$ 4.0
40 (6)	42.4 $\pm$ 3.6	0.6 $\pm$ 0.1	0.0 $\pm$ 0.0	5.9 $\pm$ 1.0	32.0 $\pm$ 1.4	81.0 $\pm$ 3.9
50 (4)	51.1 $\pm$ 14.8	1.4 $\pm$ 0.3	0.1 $\pm$ 0.0	13.5 $\pm$ 8.3	24.7 $\pm$ 6.1	90.8 $\pm$ 7.0
60 (2)	44.9 $\pm$ 3.0	0.9 $\pm$ 0.2	0.0 $\pm$ 0.0	5.8 $\pm$ 1.1	26.5 $\pm$ 3.1	78.1 $\pm$ 1.2
70 (4)	58.8 $\pm$ 6.7	0.8 $\pm$ 0.3	0.4 $\pm$ 0.3	11.3 $\pm$ 8.2	20.0 $\pm$ 2.6	92.0 $\pm$ 1.0
80 (6)	52.4 $\pm$ 7.3	0.7 $\pm$ 0.1	0.8 $\pm$ 0.5	13.4 $\pm$ 6.1	19.7 $\pm$ 1.3	87.0 $\pm$ 3.6
100 (4)	37.6 $\pm$ 10.6	0.5 $\pm$ 0.2	1.9 $\pm$ 1.8	13.6 $\pm$ 9.2	21.6 $\pm$ 6.6	89.2 $\pm$ 3.7
Average						88.3 $\pm$ 1.8

Notes: Tabulated values represent the percent of radioactive dose applied (mean  $\pm$  SE,  $n = 2-6$ ).

A = % Dose evaporated, B = % Dose penetrated.

<sup>A</sup>Ethanol rinsing of evaporation trap, modified Franz cell top and connecting tubes (where applicable).

<sup>B</sup>% dose recovered from skin and tape strip (where applicable) after 24 hr.

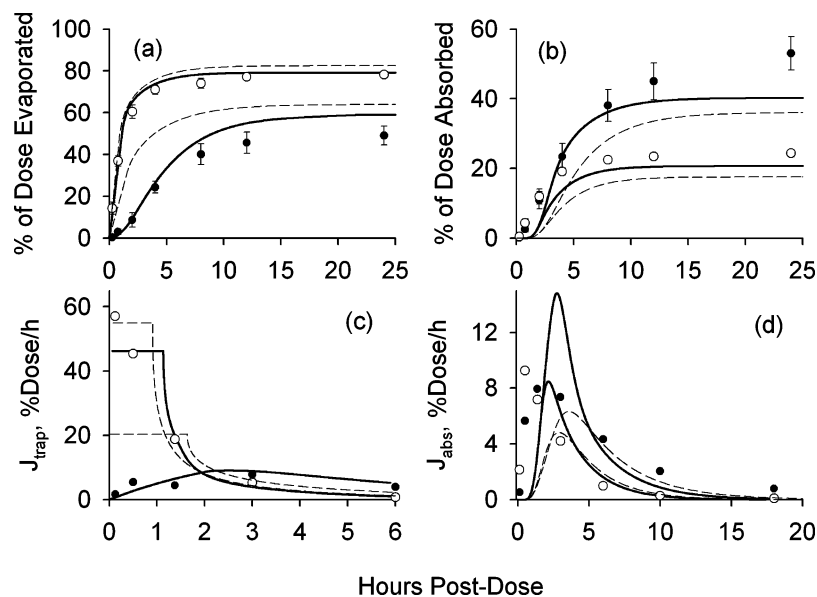


**FIGURE 3.** Skin disposition of radioactivity associated with  $^{14}\text{C}$ -DEET in the controlled airflow study. ● 30 mL/min ( $n = 4$ ), ○ 80 mL/min ( $n = 6$ ). (a) Cumulative trapped volatiles; (b) cumulative amount in receptor solution; (c) evaporation flux; (d) absorption flux. The solid curves were generated using the diffusion/evaporation model with the bolded parameters in column 5 of Table IV (Model 3). The dashed curves were *a priori* (Model 1) calculations using the parameters in column 3 of Table IV.

prompting the analysis discussed in the Appendix. Time lags for absorption through the skin were usually shorter than model predictions, as shown in Figures 3b and d. Short time lags for *in vitro* skin absorption studies have routinely been obtained in our laboratory<sup>(36,37)</sup> and may provide evidence for appendageal or shunt permeation pathways not included in the present skin absorption model. Tabulated values of the absorption and evaporation time course data for all of the airflow conditions studied are included in the online supplementary material to this article.

### Variable Dose Study

This data was presented by Santhanam et al.<sup>(24)</sup> and analyzed therein according to a one-layer diffusion model. Eighteen DEET doses ranging from 0.02–11,100  $\mu\text{g}/\text{cm}^2$  were tested. In that analysis, bench top absorption values were normalized to the fume hood equivalent by means of a multiplicative correction factor. This procedure was eliminated in the present analysis, which treated bench top and fume hood data simultaneously by adjusting the airflow ( $u$ ) associated with the test environment. Two representative time courses for absorption in the fume hood environment are shown in Figure 4. This figure shows the substantial intersubject variability that is frequently present in skin permeability measurements, along with diffusion model calculations. Significant features of the study included (1) a percentage absorption that increased with the amount of DEET applied for doses in the range 0.02–200  $\mu\text{g}/\text{cm}^2$ ; then decreased at higher doses; and (2) a diffusive time constant  $h^2/D$  that decreased with DEET dose over the range 10–1000  $\mu\text{g}/\text{cm}^2$ . The results were interpreted in terms of a mild, dose-dependent skin penetration enhancement effect of DEET.

### Location Study

The mass balance for this study was reported by Santhanam et al.<sup>(24)</sup> Total  $^{14}\text{C}$ -DEET permeated into the receptor solutions after 72 hr was  $40.9 \pm 5.2\%$  in the fume hood environment and  $72.2 \pm 4.0\%$  for the bench top experiments. The full time course of skin absorption is shown in Figure 5 and tabulated in the online supplementary material. This data was quite precise relative to those in Figure 4 as they were obtained using many

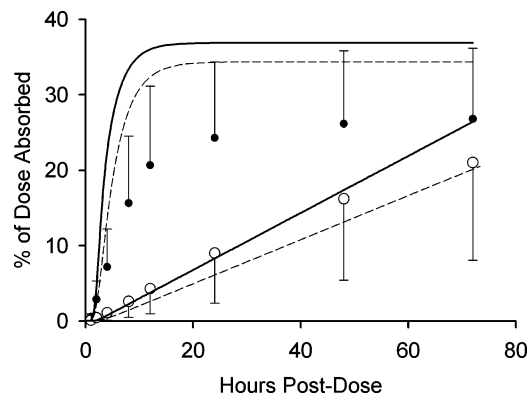


**FIGURE 4.** Skin disposition of radioactivity associated with  $^{14}\text{C}$ -DEET in the variable dose study (mean  $\pm$  SE of three donors,  $n = 3$ –4 cells per donor). ● 118  $\mu\text{g}/\text{cm}^2$ , ○ 4770  $\mu\text{g}/\text{cm}^2$ . This data represents experiments performed in the fume hood. The solid curves were generated using the diffusion/evaporation model with the bolded parameters in column 5 of Table IV (Model 3). The dashed curves were *a priori* (Model 1) calculations using the parameters in column 3 of Table IV.

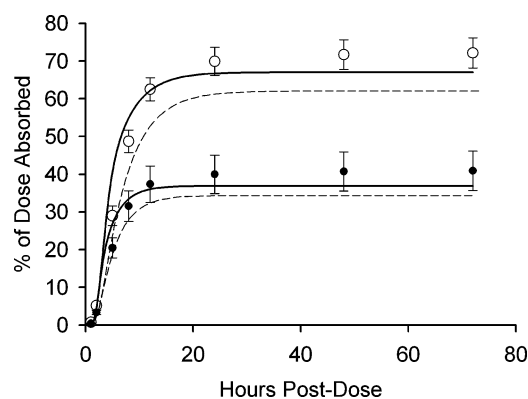


**FIGURE 5.** Skin disposition of radioactivity associated with  $^{14}\text{C}$ -DEET in the location study (mean  $\pm$  SE,  $n = 15$ ).  $\bullet$  fume hood;  $\circ$  bench top. The DEET dose was  $117 \mu\text{g}/\text{cm}^2$ , applied in  $5 \mu\text{L}$  of ethanol. The solid curves were generated using the diffusion/evaporation model with the bolded parameters in column 5 of Table IV (Model 3). The dashed curves were *a priori* (Model 1) calculations using the parameters in column 3 of Table IV.

replicates and skin from a single donor. Model calculations are shown in Figure 5.

### Test of Diffusion Model

Stratum corneum and evaporation-related transport parameters for DEET were fit to the controlled airflow, variable dose and location study data as described in Methods. The parameters resulting from this process are shown in Table IV. Default or *a priori* values for these parameters from the Excel spreadsheet, corresponding to Model 1 in this report, are provided for comparison to the fitted parameters. Representative calculations are shown in Figures 2–5.

The most significant finding from this analysis was that plausible estimates of DEET cumulative disposition on skin were provided by the spreadsheet calculation using the Model 1 transport parameters (Table II, repeated for clarity in Table IV, Column 3). The overall success of this process may be judged qualitatively by examination of the dashed curves in Figures 2–5. Quantitative measures include a squared correlation coefficient  $r^2 = 0.65$  and root mean square deviation of the calculated and observed values  $s = 12.4\%$  of dose for analysis of the full dataset of 272 observations. Thus, about 65% of the variance in the combined dataset was accounted for by Model 1. The largest deviations of the calculations from the experimental data occurred at doses above  $150 \mu\text{g}/\text{cm}^2$ , where absorption was systematically underpredicted by an average of 9% of the applied dose. The largest deviation  $[y_i(\text{obs}) - y_i(\text{fit})]$  was 31% at an applied dose of  $3160 \mu\text{g}/\text{cm}^2$ .

Least squares fitting of the stratum corneum and evaporation rate parameters (Table IV) resulted in significantly improved fits to the combined dataset as compared to Model 1. The constant diffusivity model (Model 2) led to a 2-fold reduction in the normalized sum of squared residuals  $\chi_v^2$  and a 24% reduction in rms deviation  $s$ . The variable diffusivity model (Model 3)

yielded an additional 52% reduction in  $\chi_v^2$  and a corresponding 31% reduction in  $s$ . The improvement in fit as compared with Model 2 was significant ( $p < 0.0001$ ). This was accomplished using a concentration-dependent diffusivity function (Eq. 9) for which the value of  $D_{sc}$  increased 3.4-fold over the concentration range  $0\text{--}95 \text{ mg}/\text{cm}^3$ , with 50% of the change occurring over the range  $0\text{--}38 \text{ mg}/\text{cm}^3$ . This follows from the fact that the saturation concentration ( $C_{\text{sat}}$ ) for Model 3 was  $95 \text{ mg}/\text{cm}^3$ , and the transition concentration (the inflection point of the sigmoidal curve,  $C_{\text{trans}}$ ) was 40% of  $C_{\text{sat}}$ . The use of Eq. 9 with a large value of the slope parameter,  $m = 11$ , is functionally equivalent to a step function with the step occurring at  $C_{\text{trans}}$ . It is likely that these alternative means of expressing the concentration dependence of  $D_{sc}$  would not be statistically distinguishable. However, it was evident that a steep slope (large value of  $m$ ) produced better fits to the data than a gradual slope (small value of  $m$ ). The increase in  $D_{sc}$  with concentration is consistent with observations reported elsewhere<sup>(22,24)</sup> that DEET is a mild penetration enhancer for skin. Saturation concentrations of DEET in stratum corneum ( $C_{\text{sat}}$ ) calculated from the various models ranged from  $95\text{--}182 \text{ mg}/\text{cm}^3$ , and the corresponding saturation doses ( $M_{\text{sat}}$ ) ranged from  $13\text{--}24 \mu\text{g}/\text{cm}^2$ .  $M_{\text{sat}}$  is the amount of compound required to saturate the deposition region in the SC, found in this study to be the upper 10% of the tissue; it serves as a dividing line between small and large doses in terms of skin disposition kinetics.<sup>(12)</sup>

Evaporative flux, measured at the volatiles trap in the controlled airflow study ( $J_{\text{trap}}$ ), tended to rise slowly and decay exponentially. Absorption flux ( $J_{\text{abs}}$ ) generally rose faster than model predictions but had a longer time course. These features are evident in Figure 2 and can be seen clearly in semilogarithmic plots of the flux values (data not shown). Possible explanations for the departures are provided in the next section.

## DISCUSSION

Although there is some satisfaction with being able to fit diffusion models to laboratory data, several important questions arise regarding such an exercise in the context of risk assessment: What is the range of applicability of the model? How reliable are the *a priori* (Model 1) calculations? Are there important factors that are neglected in the model that may be operative in an occupational or environmental setting? These questions are discussed below.

The diffusion model employed here and summarized in two recent book chapters<sup>(30,31)</sup> attempts to represent the transport of moderate to highly lipophilic organic permeants through human skin *in vivo* or *in vitro*. A wide range of doses may be entered, but only neat liquid chemicals or simple solutions thereof are presently parameterized. Factors such as skin thickness, temperature, hydration state, capillary clearance, and wind velocity are taken into account, but skin penetration enhancement effects other than that of water are not anticipated. Site-to-site variation in skin permeability is not addressed. Polar permeants that most likely penetrate skin by appendageal or defect pathways (e.g., salts, sugars, or

**TABLE IV. Diffusion Model Parameters Determined by Model-Fitting Procedure**

Parameter	Units	<i>a priori</i> value Model 1	Fitted Value Model 2 <sup>A</sup>	Model 3 <sup>B</sup>
Fitted parameters				
$D_0$	$\text{cm}^2\text{s}^{-1}$	$2.91 \times 10^{-11}$	$3.22 \times 10^{-11}$	<b><math>2.82 \times 10^{-11}</math></b> <sup>C</sup>
$D_{\text{sat}}/D_0$		—	—	<b>3.4</b> <sup>C</sup>
$C_{\text{trans}}/C_{\text{sat}}$		—	—	<b>0.4</b> <sup>C</sup>
$m$		—	—	<b>11</b> <sup>C</sup>
$K_{\text{sc}}$	—	18.42	14.6	<b>9.6</b> <sup>C</sup>
$k'_g$		6320	5618	<b>[5618]</b> <sup>C,D</sup>
$V'_h$	min	—	-104	<b>[-104]</b> <sup>C,D</sup>
$V_{h0}$	mL/min	—	8363	<b>[8363]</b> <sup>C,D</sup>
Derived parameters				
$h_{\text{sc}}^2/D_0$	hr	17.0	15.4	17.6
$C_{\text{sat}}$	$\text{mg}/\text{cm}^3$	182	144	95
$M_{\text{sat}}$	$\mu\text{g}/\text{cm}^2$	24.4	19.3	12.7
$k_p$	cm/hr	0.00143	0.00126	0.000728
$\chi$ (bench top)	—	0.60	0.55	0.95
$\chi$ (fume hood)		1.91	1.94	3.37
Statistics				
$n$		272	272	272
$s$	% dose	12.4	9.4	6.5
$r^2$	—	0.65	0.80	0.91
$\chi_v^2$	(% dose) <sup>2</sup>	153	87	42

<sup>A</sup>Model 2 assumes a constant diffusivity in the stratum corneum ( $D_{\text{sc}}$ ).

<sup>B</sup>Model 3 assumes that  $D_{\text{sc}}$  varies with DEET concentration according to Eq. 9.

<sup>C</sup>**Bolded** parameter values were used to generate the solid curves plotted in Figures 2–7.

<sup>D</sup>Bracket denotes that parameter value was fixed at the value obtained for Model 2.

biotechnology products) are not within the scope of the present program. Our laboratory plans to remove these limitations through continued development.

Most of the “predictions” from the diffusion model to date have involved a comparison to data obtained in our laboratory. Figures 6 and 7 demonstrate the plausibility of the values calculated for DEET in other laboratory settings. In both cases DEET evaporation rates calculated from the diffusion model are compared with values measured by other investigators. Figure 6 shows a comparison for a small dose study on human volar forearm *in vivo*,<sup>(19)</sup> whereas Figure 7 shows results for a considerably larger dose applied to human skin *in vitro*.<sup>(18)</sup> These two doses encompass the range of typical environmental and occupational exposure. The airflow velocity used by Spencer (Figure 6) falls in the range of typical airflow velocities (0.165–0.72 m/s) that corresponds to 11–34 mL/min in terms of our experimental apparatus. The airflow velocity (0.08 m/s) used to generate the theoretical curves in Figure 7 was optimized to fit the data because the rate was not given in the reference.

The largest uncertainty in making specific comparisons of this nature is the appropriate value of the evaporation mass transfer coefficient under various conditions. In the context of the mass transfer model employed herein (Eqs. 4–8) this amounts to determining the appropriate value of

the wind velocity  $u$ . For the comparisons shown, the value of  $u$  used in preparing Figure 6 was easily related to the experimental conditions, whereas that used for Figure 7 was not. The experimental evaporation rate in the latter study was surprisingly low. The subject of evaporation mass transfer coefficients for occupational settings was reviewed by Nielsen et al.<sup>(38)</sup> and remains a subject of research.

It is worth noting that the evaporation rate associated with the Model 1 calculation (dashed curve) in Figure 6 lies below that of the Model 3 calculation (solid curve), whereas in Figure 7 the situation is reversed. This is not a mistake. The interchange occurs as a result of the widely different doses associated with the two experiments. The Spencer et al. study (Figure 6) was conducted at a dose of  $25 \mu\text{g}/\text{cm}^2$ , very close to the dose required to saturate the upper stratum corneum,  $M_{\text{sat}}$  (cf. Table IV). At this dose the 2-fold higher skin permeability  $k_p$  in the Model 1 calculation vs. Model 3 led to a higher absorption rate and, consequently, a lower evaporation rate from the residual permeant in the skin. The Reifenrath and Robinson study (Figure 7) employed a dose of  $300 \mu\text{g}/\text{cm}^2$ , well above the saturation dose  $M_{\text{sat}}$ . In this case (Case 2 according to the terminology in Ref. 12), a liquid DEET film persisted on the skin surface for a substantial period of time—more than 11 hr according to the calculations shown in Figure 7.

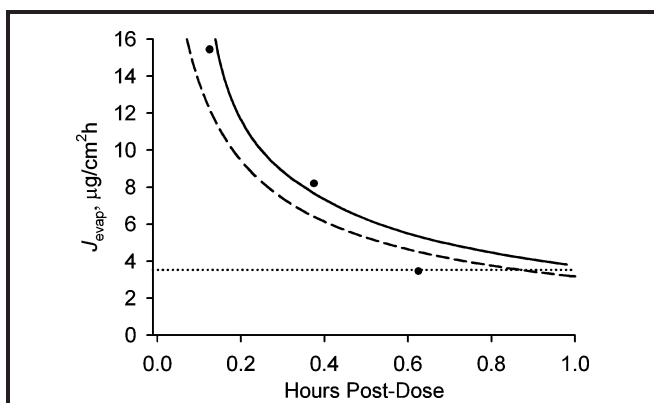


**FIGURE 6.** DEET evaporation rates under an airflow of 30 mL/min following a 25  $\mu\text{g}/\text{cm}^2$  dose in ethanol to human volar forearm *in vivo* (mean  $\pm$  SD,  $n = 7$ ).<sup>(19)</sup> The data is plotted at the midpoint of the collection interval. The dotted line marks the evaporation rate during the 30–35 min interval, reported by these investigators to be the interval associated with a minimum effective evaporation rate for repellency. The solid curves were generated using the diffusion/evaporation model with the bolded parameters in column 5 of Table IV (Model 3). The dashed curves were *a priori* (Model 1) calculations using the parameters in column 3 of Table IV. They were calculated using  $v = 30 \text{ mLmin}^{3/4l}$ , corresponding to a wind velocity  $u = 0.61 \text{ ms}^{3/4l}$  (Table II).

The evaporation rate in this case is given by  $k_{\text{evap}}\rho$  (Eq. 4), which was larger for the Model 1 calculation due to the higher value of  $k'_g$  (Table IV).

Much less is known about the reliability of transient skin absorption calculations than is known about steady-state skin permeability. For the latter, the best current correlations for the extended Flynn database<sup>(29)</sup> yield a root mean square error in  $\log_{10}(\text{permeability})$  of about 0.51 log units and a maximum error of 0.72 log units. These values correspond approximately to arithmetic factors of 3 and 5, respectively. It seems unlikely that transient skin absorption calculations employing transport

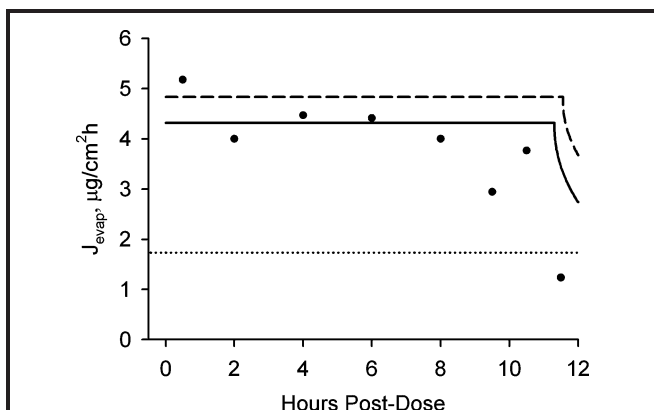


**FIGURE 7.** Mean DEET evaporation rate from human skin *in vitro* under an airflow of 30 mL/min following a 300  $\mu\text{g}/\text{cm}^2$  dose.<sup>(18)</sup> The solid and dashed curves were generated as in Figure 6 using  $v = 6 \text{ mL/min}$ , corresponding to  $u = 0.08 \text{ m/sec}$ . The dotted line is the minimum effective evaporation rate for repellency reported by Reifenrath and Robinson.<sup>(18)</sup>

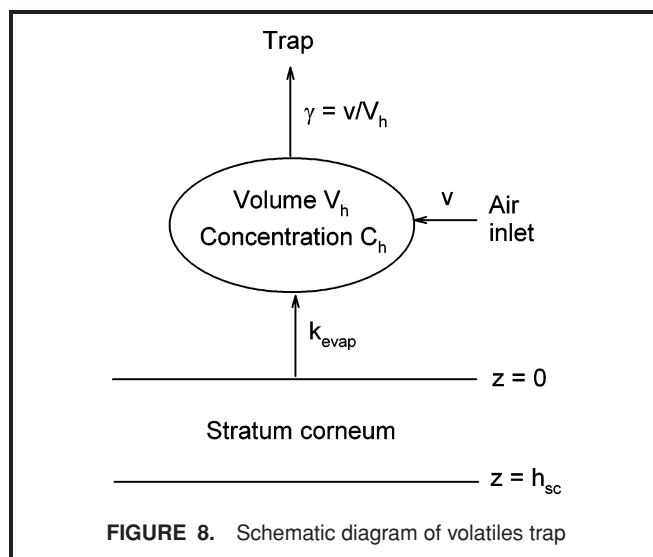


**FIGURE 8.** Schematic diagram of volatiles trap

parameters derived only from physical properties will improve on the steady-state results. However, it is quite possible to use steady-state absorption data to improve the estimates of transport parameters for transient absorption.<sup>(13,29)</sup> The present spreadsheet calculation implements such a scheme. In other words, an experimental skin permeability coefficient entered by the user overrides the estimated permeability coefficient calculated in the spreadsheet. The combination of a steady-state permeability experiment with a model for transient diffusion may lead to predictions considerably better than the typical 3-fold uncertainty in steady-state permeation rates. This remains to be shown.

Some details of the laboratory results with DEET were not anticipated by model calculations. The large delay time for vapor trapping at low airflows in the controlled airflow study was one of these features. It was treated in the model by the procedure outlined in the Appendix. A second such feature was the prolonged “tail” of some absorption and evaporation rate profiles, especially those associated with high DEET doses. This feature also was seen in a previous study of benzyl alcohol in both skin and silicone membrane.<sup>(8)</sup> It appears to contradict the theoretical prediction of a terminal exponential decay for diffusion in one dimension.<sup>(12,16)</sup> We suggest that diffusion of DEET into the skin clamped beneath the ground glass joint, followed by a slow release from this compartment, may be responsible for this phenomenon. The magnitude of this effect was not large enough to appreciably affect the cumulative release profile; however, it might become important were one using the diffusion cell methodology to predict the duration of effective repellency. The model calculation, of course, experiences no such artifact.

Several additional factors must be considered when applying skin absorption models to occupational settings. Skin condition, body site, degree of occlusion, and decontamination efforts or lack thereof all affect absorption of the chemicals with which workers come into contact. A range of exposure scenarios is thus encountered. A proven, but data-intensive way

of addressing these issues is to first develop probability profiles for the factors most relevant to skin absorption, then use them as inputs for a stochastic calculation of risk. The deterministic model provides the link between the exposure variables and the outcome of the process—in this case, systemic absorption. The optimum use of these calculations in systemic risk assessment may well come from such a combination of tools. The related problem of skin sensitization risk assessment is discussed elsewhere.<sup>(1)</sup> The spreadsheet skin absorption model is available from the authors on request.

## CONCLUSIONS

Many features of the dose and airflow dependence of DEET disposition on human skin *in vitro* can be described using the finite dose diffusion model discussed in this report. *A priori* (Model 1) calculations containing no fitted parameters described cumulative DEET absorption profiles to within an rms error of 12.4% of the applied dose under a variety of conditions. Optimized parameters including a concentration-dependent diffusivity in the stratum corneum reduced this error to 6.5%. The analysis supported the conclusion drawn previously that DEET is a mild penetration enhancer for skin. The spreadsheet implementation of the diffusion model opens the door for use of this method in occupational hygiene.

## ACKNOWLEDGMENTS

DEET protein binding measurements were skillfully conducted by Rania Ibrahim. Financial support for this study was provided by NIOSH/CDC grant R01 OH007529. The conclusions reached represent the opinions of the authors and have not been endorsed by NIOSH.

## REFERENCES

1. **Basketter, D.A., C.K. Pease, G.B. Kasting, et al.:** Skin sensitisation and epidermal disposition. The relevance of epidermal bioavailability for sensitisation hazard identification/risk assessment. *Alt. Lab. Animals* 35:137–154 (2007).
2. **Buchwald, P., and N. Bodor:** A simple, predictive, structure-based skin permeability model. *J. Pharm. Pharmacol.* 53:1087–1098 (2001).
3. **Johnson, M.E., D. Blankschtein, and R. Langer:** Evaluation of solute permeation through the stratum corneum: Lateral bilayer diffusion as the primary transport mechanism. *J. Pharm. Sci.* 86(10):1162–1172 (1997).
4. **Moss, G.P., J.C. Dearden, H. Patel, and M.T.D. Cronin:** Quantitative structure-permeability relationships (QSPRs) for percutaneous absorption. *Toxicol. in Vitro* 16:299–317 (2002).
5. **Lyman, W.J., W.F. Reehl, and D.H. Rosenblatt:** *Handbook of Chemical Property Estimation*. New York: McGraw-Hill, 1982.
6. **Potts, R.O., and R.H. Guy:** Predicting skin permeability. *Pharm. Res.* 9(5):663–669 (1992).
7. **Scheuplein, R.J., and L. Ross:** Effects of surfactants and solvents on the permeability of epidermis. *J. Soc. Cosmet. Chem.* 21:853–873 (1970).
8. **Miller, M.A., V. Bhatt, and G.B. Kasting:** Absorption and evaporation of benzyl alcohol from skin. *J. Pharm. Sci.* 95(2):281–291 (2006).

9. **Blank, I.H., J. Moloney, A.G. Emslie, I. Simon, and C. Apt:** The diffusion of water across the stratum corneum as a function of its water content. *J. Invest. Dermatol.* 82:183–194 (1984).
10. **Kasting, G.B., N.D. Barai, T.-F. Wang, and J.M. Nitsche:** Mobility of water in human stratum corneum. *J. Pharm. Sci.* 92(11):2326–2340 (2003).
11. **Wilschut, A., W.F. ten Berge, P.J. Robinson, and T.E. McKone:** Estimating skin permeation. The validation of five mathematical skin penetration models. *Chemosphere* 30(7):1275–1296 (1995).
12. **Kasting, G.B., and M.A. Miller:** Kinetics of finite dose absorption through skin 2. Volatile compounds. *J. Pharm. Sci.* 95(2):268–280 (2006).
13. **Frasch, H.F., and A.M. Barbero:** The transient dermal exposure: Theory and experimental(RUN INI)examples using skin and silicone membranes. *J. Pharm. Sci.* 97(4):1578–1592 (2008).
14. **Bhatt, V.:** “Absorption and Evaporation of Pesticides from Human Skin.” Ph.D. Dissertation, College of Pharmacy, University of Cincinnati, 2007.
15. **Ray Chaudhuri, S.:** “Mathematical Modeling of Percutaneous Absorption of Volatile Compounds Following Transient Liquid-Phase Exposures.” Ph.D. dissertation, Chemical and Materials Engineering, University of Cincinnati, 2007.
16. **Anissimov, Y.G., and M.S. Roberts:** Diffusion modeling of percutaneous absorption kinetics: 2. Finite vehicle volume and solvent deposited solids. *J. Pharm. Sci.* 90:504–520 (2001).
17. **McCarley, K.D., and A.L. Bunge:** Pharmacokinetic models of dermal absorption. *J. Pharm. Sci.* 90:1699–1719 (2001).
18. **Reifenrath, W.G., and P.B. Robinson:** In vitro skin evaporation and penetration characteristics of mosquito repellents. *J. Pharm. Sci.* 71:1014–1018 (1982).
19. **Spencer, T.S., J.A. Hill, R.J. Feldmann, and H.I. Maibach:** Evaporation of diethyltoluamide from human skin in vivo and in vitro. *J. Invest. Dermatol.* 72(6):317–319 (1979).
20. **Selim, S., R.E. Hartnagel, T.G. Osimitz, K.L. Gabriel, and G.P. Schoenig:** Absorption, metabolism, and excretion of N,N-diethyl-m-toluamide following dermal application to human volunteers. *Fundam. Appl. Toxicol.* 25:95–100 (1995).
21. **Qui, H., H.W. Jun, and J.W. McCall:** Pharmacokinetics, formulation and safety of insect repellent N,N-diethyl-3-methylbenzamide (deet): A review. *J. Am. Mosquito Contr. Assoc.* 14(1):12–27 (1998).
22. **Windheuser, J.J., J.L. Haslam, L. Caldwell, and R.D. Shaffer:** The use of N,N-diethyl-m-toluamide to enhance dermal and transdermal delivery of drugs. *J. Pharm. Sci.* 71:1211–1213 (1982).
23. **Baynes, R.E., Halling, K. B., and J.E. Riviere:** The influence of diethyl-m-toluamide (DEET) on the percutaneous absorption of permethrin and carbaryl. *Toxicol. Appl. Pharmacol.* 144(2):332–339 (1997).
24. **Santhanam, A., M.A. Miller, and G.B. Kasting:** Absorption and evaporation of N,N-diethyl-m-toluamide (DEET) from human skin in vitro. *Toxicol. Appl. Pharmacol.* 204:81–90 (2005).
25. **Saiyasombati, P., and G.B. Kasting:** Disposition of benzyl alcohol following topical application to human skin in vitro. *J. Pharm. Sci.* 92(10):2128–2139 (2003).
26. **Monteith, J.L., and M.H. Unsworth:** *Principles of Environmental Physics*. 2nd ed., Oxford: Butterworth-Heinemann, 1990.
27. **Nitsche, J.M., T.-F. Wang, and G.B. Kasting:** A two-phase analysis of solute partitioning into the stratum corneum. *J. Pharm. Sci.* 95(3):649–666 (2006).
28. **Wang, T.-F., G.B. Kasting, and J.M. Nitsche:** A multiphase microscopic model for stratum corneum permeability. I. Formulation, solution and illustrative results for representative compounds. *J. Pharm. Sci.* 95(3):620–648 (2006).
29. **Wang, T.-F., G.B. Kasting, and J.M. Nitsche:** A multiphase microscopic model for stratum corneum permeability. II. Estimation of physicochemical parameters and application to a large permeability database. *J. Pharm. Sci.* 96(11):3024–3051 (2007).
30. **Kasting, G.B., M.A. Miller, and J.M. Nitsche:** Absorption and evaporation of volatile compounds applied to skin. In *Dermatologic, Cosmeceutic*

- and *Cosmetic Development*, K.A. Walters and M.S. Roberts (eds.). New York: Informa Healthcare USA, 2008. pp. 385–400.
31. **Nitsche, J.M., and G.B. Kasting:** Biophysical models for skin transport and absorption. In *Dermal Absorption and Toxicity Assessment*, 2nd ed., M.S. Roberts and K.A. Walters (eds.). New York: Informa Healthcare USA, 2008. pp. 249–267.
  32. **Kretsos, K., M.A. Miller, G. Zamora-Estrada, and G.B. Kasting:** Partitioning, diffusivity and clearance of skin permeants in mammalian dermis. *Int. J. Pharm.* 346(1–2):64–79 (2008).
  33. **Bevington, P.R.:** *Data Reduction and Error Analysis for the Physical Sciences*. New York: McGraw-Hill, 1969.
  34. **Saiyasombati, P., and G.B. Kasting:** Two-stage kinetic analysis of fragrance evaporation and absorption from skin. *Int. J. Cosmet. Sci.* 25:235–243 (2003).
  35. **Saiyasombati, P., and G.B. Kasting:** Evaporation of benzyl alcohol from human skin in vivo. *J. Pharm. Sci.* 93(2):515–520 (2004).
  36. **Kasting, G.B.:** Kinetics of finite dose absorption 1. Vanillylnonanamide. *J. Pharm. Sci.* 90(2):202–212 (2001).
  37. **Kasting, G.B., M.M. Miller, and P.S. Talreja:** Evaluation of stratum corneum heterogeneity. In *Percutaneous Absorption*, 4th ed., R.L. Bronaugh and H.I. Maibach (eds.). New York: Taylor & Francis, 2005. pp. 193–212.
  38. **Nielsen, F., E. Olsen, and A. Fredenslund:** Prediction of isothermal evaporation rates of pure volatile organic compounds in occupational environments — A theoretical approach based on laminar boundary layer theory. *Ann. Occup. Hyg.* 39(4):497–511 (1995).
  39. **Dahlquist, G., and A. Bjork:** *Numerical Methods*. Englewood Cliffs, N.J.: Prentice Hall, 1974.

## APPENDIX

### Headspace Delay for Controlled Airflow Experiments

The controlled airflow study involved the use of an enclosed top for the Franz cells fitted with a Tenax absorbent cartridge, through which room air was drawn by a precision air pump. The system has been previously described.<sup>(25)</sup> The headspace associated with this trap introduced a delay between the time <sup>14</sup>C-DEET evaporated from the skin surface and the time it arrived in the absorbent cartridge. The delay was noted in the earlier study of benzyl alcohol,<sup>(25)</sup> but it was of minor significance for this relatively volatile compound and details of the analysis were not provided. A much more significant delay was encountered for DEET. The delay was accounted for in the analysis by a well-stirred compartment approach incorporating a variable headspace volume, as follows.

The trapping apparatus was envisioned as shown in Figure 8. Volatiles from the skin surface ( $z = 0$ ) evaporate from the skin surface into a well-stirred compartment of volume  $V_h$ . The evaporation rate per unit of surface area is given by

$$J_{\text{evap}}(t) = k_{\text{evap}}C(0, t) \quad (\text{A1})$$

so that the total evaporation rate for a surface of area  $A$  is  $J_{\text{evap}}(t) \cdot A$ . The headspace concentration  $C_h$  is considered to be low so that condensation of the volatiles back onto the skin surface may be neglected. A constant airflow of magnitude  $v$  passes through the headspace and deposits the volatile ingredient(s) into the trap at a rate given by

$$J_{\text{trap}} = vC_h = \gamma M_h \quad (\text{A2})$$

where  $M_h$  is the amount of the ingredient in the headspace and  $\gamma = v/V_h$ . Mass balance on the headspace then requires that

$$\frac{dM_h}{dt} = J_{\text{evap}}(t) \cdot A - \gamma M_h \quad (\text{A3})$$

or

$$\frac{dM_h}{dt} + \gamma M_h = J_{\text{evap}}(t) \cdot A \quad (\text{A4})$$

Equation A4 may be solved by Laplace transforms to yield

$$M_h(t) = A \int_0^t J_{\text{evap}}(\tau) e^{-\gamma(t-\tau)} d\tau. \quad (\text{A5})$$

Substituting Eq. A4 into Eq. A2 yields the flux into the trap:

$$J_{\text{trap}}(t) = \gamma A \int_0^t J_{\text{evap}}(\tau) e^{-\gamma(t-\tau)} d\tau. \quad (\text{A6})$$

The cumulative amount of the ingredient deposited in the trap at time  $t$  is

$$M_{\text{trap}}(t) = \int_0^t J_{\text{trap}}(t') dt' \quad (\text{A7})$$

The spreadsheet calculation solves partial differential equations within the skin layers to yield  $C(0, t)$  and, hence,  $J_{\text{evap}}(t)$  according to Eq. A1. Equation A6 was then integrated numerically using the implicit trapezoidal rule<sup>(39)</sup> to yield  $J_{\text{trap}}$ , which was further integrated according to Eq. A7 to yield  $M_{\text{trap}}$ . At times long compared with the headspace time constant  $1/\gamma$ , this solution was numerically unstable due to the growth of an undesired positive exponential term that was difficult to suppress. This difficulty was overcome by noting that the ratio of  $J_{\text{trap}}$  to  $J_{\text{evap}}$  became constant for  $t \gg 1/\gamma$ . Hence, Eq. A6 was integrated until a predetermined transition time  $t_{\text{trans}}$ , after which  $J_{\text{trap}}$  was calculated as

$$J_{\text{trap}} = kJ_{\text{evap}} \quad (\text{A8})$$

where  $k$  was the ratio of  $J_{\text{trap}}$  to  $J_{\text{evap}}$  at time  $t_{\text{trans}}$ . Experience showed that the choice of  $t_{\text{trans}} = 15/\gamma$  led to an accurate and stable solution. This transition time was reset to the current time  $+ 15/\gamma$  when conditions on the skin surface changed abruptly, i.e., as the liquid film of DEET disappeared. This condition marks the transition between a large dose (Case 2) and a small dose (Case 1) according to the diffusion model.<sup>(12)</sup>

Equations A1 to A8 provided a mechanism for describing the kinetics of the vapor collection process at any particular value of the airflow  $v$ . However, analysis showed that the value of the headspace volume  $V_h$  required to describe the trap kinetics for DEET was much larger than the physical volume of the diffusion cell (about 3–5 mL). Furthermore, delay times increased disproportionately with decreasing airflow, requiring larger values of  $V_h$  for lower airflows. Least squares fitting of the optimum  $V_h$  values at each airflow over the range 20–80 mL/min (excluding one high value at  $v = 50$  mL/min) to a

linear function lead to the relationship

$$\begin{aligned} V_h &= 8363 - 104v \quad 20 \leq v \leq 80 \\ n &= 6; s = 345; r^2 = 0.977 \end{aligned} \quad \text{(A9)}$$

where  $v$  is expressed in mL/min and  $V_h$  in mL. In Table IV, Eq. A9 is expressed as  $V_h = V_{h0} + V_h^{\phi} \times v$ ; thus,  $V_{h0} = 8363$  and  $V_h^{\phi} = 3/4 104$ . Because the volume of the apparatus does not actually vary with airflow, the variation may be alternatively thought of as a condensed film of thickness  $\delta$  that forms on the inner surfaces of the apparatus. This is plausible because the glass top of the diffusion cell was not heated and thus had a temperature lower than the skin surface. Geometrical considerations assuming the trap to be a perfect cylinder showed that the maximum values of  $\delta$  equivalent to

the headspace volumes calculated from Eq. A9 ranged from 0.02 nm at 80 mL/min to 27 nm at 20 mL/min. Thus, a very thin condensed film of DEET would account for a large effective headspace volume.

Equations A1 to A9 were used to describe the observed evaporation kinetics for the controlled airflow study reported in the main text. This mathematical treatment does not affect the calculated evaporation rate from the skin surface or the cumulative amounts evaporated or absorbed after times much longer than the vapor trap time constant  $1/\gamma$ . This treatment is thus an elaboration required to explain the results of vapor trapping experiments that was not required for unoccluded exposures. Consequently it was not applied to the variable dose or location study results.